



Research Article

**IMPLEMENTATION OF SENSORLESS POSITION DETECTION CIRCUIT WITH FOUR-SWITCH INVERTER TOPOLOGY FOR A PERMANENT MAGNET SYNCHRONOUS MOTOR**

**Fatih SEREZ<sup>1</sup>, Burcu ERKMEN\*<sup>2</sup>**

<sup>1</sup>*Arçelik, ISTANBUL; ORCID: 0000-0002-1507-6134*

<sup>2</sup>*Yıldız Technical University, Electronics and Communications Engineering Department, Esenler-ISTANBUL; ORCID: 0000-0002-5581-9764*

**Received: 11.11.2019 Revised: 26.12.2019 Accepted: 06.02.2020**

**ABSTRACT**

Applications using permanent magnet synchronous motors (PMSM) are becoming increasingly popular today. These motors are controlled by special electronic circuits; with the advances in semiconductor technologies, they have acquired more specialized and extensive application areas. In this study, the sensorless position detection was performed with six step control of a PMSM / BLAC motor using four switch inverter topology. In the method that used, as the necessary commutation points for motor driving are obtained directly at the developed circuit output, the 30° electrical phase shifting was not required, as in the methods based on the back-EMF voltage. Shifting is performed depending on delaying of the filters adapted to the circuit and the motor speed. The motor terminal voltages are used in the application with respect to the ground point of the circuit without the need for a motor neutral point. Thus, when the PMSM / BLAC motor is driven by four switches and six step control, sensorless position detection is performed to provide position input to the closed loop speed control with fewer circuit components, less drive complexity and cost effectiveness.

**Keywords:** BLAC motor, four-switch inverter, permanent magnet synchronous motor, PMSM, position detection, six step control, trapezoidal control.

**1. INTRODUCTION**

PMSMs controlled by the electronic circuits have found increasingly extensive application areas nowadays because of the development and cost of digital controller (MCU, DSP, etc.) circuit element technologies. It has become possible to make motor control applications with fewer elements owing to the development of processors with more memory and processing capacity in the unit time. The sensorless motor control is of interest for manufacturers in the academy as well as in the industry. Furthermore the energy efficiency and the environmental awareness issues gained importance and entered into daily life with legal regulations. Thus, the permanent magnet synchronous motor control applications are frequently seen in areas such as industry, automotive, medical and home appliance.

The carried out studies for PMSM / BLAC motors related with motor drive design, four switch inverter topologies, position detection circuits and the control strategies are available in the

\* Corresponding Author: e-mail: bkapan@yildiz.edu.tr, tel: (212) 383 59 18

literature. In the study [1], the transmission control of the switches in the inverter is based on the calculation of the harmonic current coefficients using the Fourier series coefficients revealed by the speed controller. By comparing these current values with the instant current values and the back-EMF; the drive signal is produced by the PI controller at the appropriate duty ratio. In [2], switching was performed by sensing the current passing through the DC-link center point by the sensor. In order to improve the controller performance and the speed adjustment, an adaptive PI algorithm with single neuron was performed [2], [3]. Due to the nature of the low resolution of position detection, the speed feedback should be sampled inconstant. In [4], fuzzy logic gain PI control was proposed. In order to improve the transient response characteristics of the system, a new speed control method was used in [5] using acceleration feed forward compensation and disturbance torque estimation method.

In PMSMs, commutation is obtained by using the motor phase voltages. The noise is eliminated with the 2nd degree butterworth active filter [6] and the low-pass filter [7]. With the existing filter time delays, zero crossing points are obtained, so that the commutation is provided. There is also no need for a phase shifting operation. In [8], for the control strategy using the current sensor, the working process of the BLDC motor are divided into 6 modes. This method is based on detecting the zero crossing points of the three voltage functions derived from the difference of the motor phase voltages measured from the motor terminals. In [9], the relation between the current slope differences is derived by using four-switch inverter topology and expressed in 24 transform matrices.

The dynamic and the constant torque-speed control of the PMSMs is provided by PWM produced by different techniques. Stator feed forward dq-axes voltage control algorithm has been introduced in [10] to achieve simple, effective and low cost control scheme. In [11] a new speed-current single-loop control method based on the Port Controlled Hamiltonian theory and disturbance observer which is easy to be implemented on a real-time platform, has been proposed for the PMSM drive system. In [12], a new asymmetric PWM is proposed to perform six commutations for BLDC motor drive with four-switch three-phase (FSTP) inverters and to detect the back-EMFs by generating the idle four-phase voltage. The direct torque control and the 4 switch topology were adapted with mathematical transformations and similar results to 6 step control were obtained in [13]. The technique proposed in [14] is based on a strategy in which the current slopes of the rising and decaying phases along the commutation intervals can be equalized with the appropriate duty cycle in the commutations. The commutation signals are obtained from the zero crossing points of the three voltage functions, derived from filtered stator terminal voltages, connected to the inverter circuit including active power switch in [15]. The average terminal voltages are controlled using the direct phase current control method. In order to achieve the dynamic and constant torque-speed characteristics of the four-switch BLDC motor drive, there are studies for direct-current-controlled PWM generation in [16] and in [17]. In order to take full advantage of embedded controllers, operating as a motor drive and including DC-link voltage balancing control is implemented on digital signal processing (DSP) [18]. In [19], a Field Programmable Gate Arrays (FPGA) is implemented for a four-level active-clamped converter to drive the PMSM, a DC-link voltage balancing closed-loop control (VBC), and a virtual-vector-based modulator in order to reduce cost and duty ratios. Some of the studies in the literature are aimed to diagnose various faults in the PMSM's drive system. A new fault detection algorithm is presented in [20]. The drive system after the fault identification is reconfigured by four-switch topology connecting a faulty leg to the middle point of DC-link using bidirectional switches. In the other study [21], the fault detection is made by phase current and voltage changes between lower legs and middle point of DC-link. After the fault detection, the drive system is reconfigured by the FSTP (four-switch three-phase) topology. In [22], a new fault-tolerant method for open-phase PMSM is proposed. A novel transformation matrix for current/voltage references is designed in the d-q frame to obtain stronger fault-tolerance capability.

In this work; design and experimental studies of a PMSM for sensorless position detection by

using four switch inverter topologies are realized. Unlike the previous studies in the literature, instead of approaches and mathematical complexities for BLAC sensorless speed control methods (FOC), the sensorless position detection using the four-switch inverter topology of the three-phase PMSM with the sinus back-EMF was performed by 6-step trapezoidal control method. The position detection method has been verified by using the closed loop speed control of the motor. So, it provides position input to the closed loop speed control with fewer circuit components, less drive complexity and cost effectiveness.

## **2. SENSORLESS FOUR-SWITCH BLDC/PMSM MOTORS**

Sensorless motor control, reduction of inverter losses, control with one or three shunt resistors, using of PGAs in motor control attracts the attention of manufacturers in the industry as well as academia. Thus, the PMSM control applications in industry, automotive, medical and home appliance are becoming more common today.

The sensorless motor control studies are based on the induction of a voltage depending on the rotor position at the phase terminals during the rotational movement of the brushless motors. In the literature, the back-EMF based methods, flux estimation based methods, methods based on stator inductance changes, observer based methods and intelligent control methods can be used for position detection [7]. In the Back-EMF based position method, in the excitation of a three-phase BLDC motor, except for the phase-commutation periods, only two of the three phase windings are conducting at a time and the other phase contains the back-EMF information. The position information required for the commutation is sensed by the aid of electronic circuits.

The sensorless speed control of the PMSMs can be performed in multiple different ways such as closed loop speed control and field-oriented control (FOC) widely used in the industry. The number of active switches during space vector modulation (SVM) included commutation is greater than the 6-step control in the BLDC motor. Therefore, the conduction and switching power losses on the inverter stage are higher and additional heatsink is required for properly working of the power switch. Considering these effects, the use of less power in the PMSM's speed control has gained importance. In this work, a position detection method for 6-step control of PMSM is presented by using four switch inverter topology.

### **2.1. PMSM Motor Theory**

In the literature, for 6-switch three-phase PMSM speed control, the average voltage is calculated to reach the required speed at the time of  $60^\circ$  electrical commutation [23]. This process is done in  $360^\circ$  electrical movement of the motor and in 6 different commutation regions. The average voltage is calculated by using 6 different combinations of upper and lower switch pairs in different legs. In the 4-switch inverter topology shown in Figure 1, the DC bus voltage is obtained by two identical capacitors connected to each other in series. One phase of PMSM is connected to their midpoint. An upper and a lower switch of the inverter is discarded so that the inverter bridge is created by using 4 switches. The middle ends of the inverter is connected the remaining terminals of the motor.

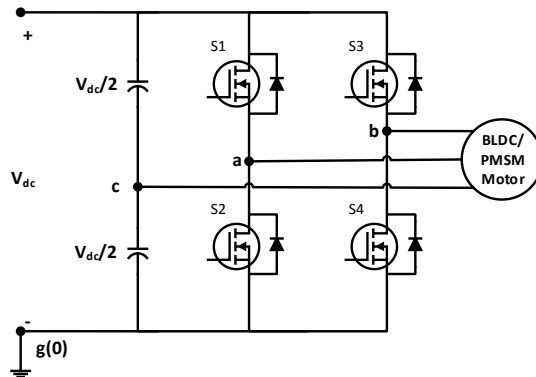


**Figure 1.** Four switch sensorless PMSM inverter topology

The terminal voltages of the 3-phase PMSM with a four switch inverter topology are given in Equation 1, 2, 3. The explanations of the electrical parameters given in the equations are shown in Table 1.

$$V_{ag} = R \cdot i_a + L \cdot \frac{di_a}{dt} + e_{an} + V_{ng} \tag{1}$$

$$V_{bg} = R \cdot i_b + L \cdot \frac{di_b}{dt} + e_{bn} + V_{ng} \tag{2}$$

$$V_{cg} = R \cdot i_c + L \cdot \frac{di_c}{dt} + e_{cn} + V_{ng} \tag{3}$$

**Table 1.** Three Phase PMSM electrical parameters

$V_a, V_b, V_c$	Terminal Voltages
$V_n$	Motor Star-Point Voltage
$V_g$	Circuit reference point voltage
R	Stator phase resistance
L	Stator phase inductance
$i_a, i_b, i_c$	Stator phase currents
$e_a, e_b, e_c$	Back EMFs, induced in the stator windings

In the 6-step control, two phases are energized in each commutation. Therefore, the currents in these phases are equal amplitude but the current in the remaining phase is zero. A 60° electrical angle is formed between the  $V_{ag}$  and  $V_{bg}$  voltage vectors by using this inverter topology. As a result; the  $V_{ag}$  and  $-V_{bg}$  voltage vectors are 30° electrically behind the  $e_{an}$  and  $e_{cn}$  vectors respectively. However, the  $V_{ba}$  voltage vector (or  $V_{bg}-V_{ag}$ ) is 30° electrically behind the  $e_{cn}$  vector. The PMSM inverter stator phase-to-phase voltage vectors for 6-step control with 4 switches explained in [24] are shown in Figure 2.

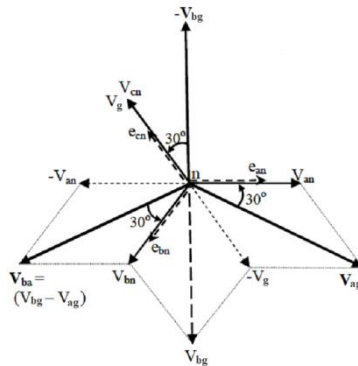


Figure 2. Inverter stator phase-to-phase voltage vectors

In order to obtain Virtual Hall Effect sensor signals, the motor phase voltages are converted to lower voltage levels by using the voltage divider circuits.

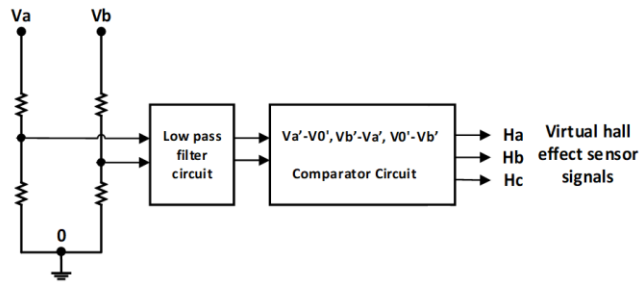


Figure 3. Sensorless position detection circuit

The Low-pass filtering is applied to the PWM signal to remove high frequency components. As the motor speed increases, the frequencies of the measured signals will also increase. The signals are then compared each other after the filtering process.

If the  $\{V_a'g - V_c'g\}$ ,  $\{V_b'g - V_a'g\}$ ,  $\{V_c'g - V_b'g\}$  values are greater (less) than zero at the end of the comparison process, it forms the logic 1 (0) at the virtual sensor signals ( $H_a$ ,  $H_b$ ,  $H_c$ ) as shown in Figure 3. Thus, three virtual Hall Effect sensor signals with  $120^\circ$  electric phase difference are obtained in square wave form.

Table 2. Sensorless PMSM commutation states for four switch inverter topology

States	$H_a$ $V_a' > V_0'$	$H_b$ $V_b' > V_a'$	$H_c$ $V_a' > V_0'$	Active Switches	Active Phases
1	1	1	0	S1	A,C
2	1	0	0	S1,S4	A,B
3	1	0	1	S4	C,B
4	0	0	1	S2	C,A
5	0	1	1	S2,S3	B,A
6	0	1	0	S3	B,C

### 3. PMSM DRIVE STAGE - SYSTEM HARDWARE DESIGN

System hardware shown in the Figure 4 composes of the following sub-circuit blocks: AC Input & Rectifier, DC Bus Voltage Reading Circuit, Switched Mode Power Supply (SMPS), Gate Driver Circuit, Power Switches for Motor Drive, Motor Back-EMF Circuit, Phase Shifting Circuit, Comparator Circuit and Microcontroller. Table 3 shows the sensorless motor control parameters.

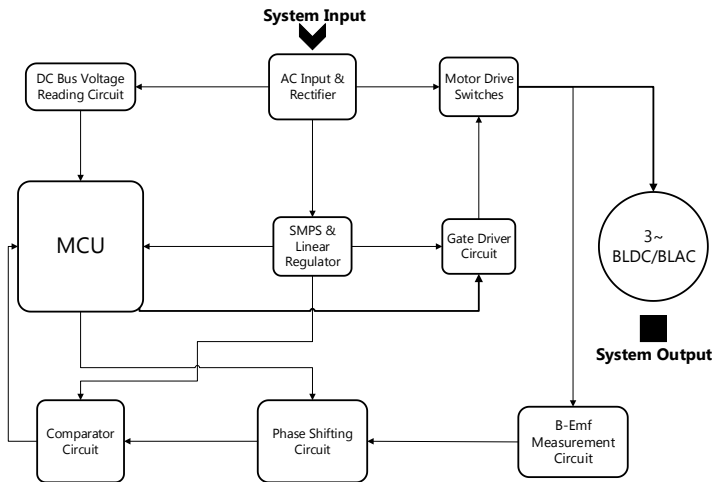


Figure 4. System hardware

Table 3. Sensorless BLAC motor control parameters

Control methods	6- step commutation, 4 switch
Position sensing	PMSM b-emf based
Switching frequency	7 kHz
PI Control Frequency	50 Hz
Speed Range	2000-3000 rpm
Number of Pole-pair (2p)	8

#### 3.1. AC Input & Rectifier Circuit

Input supply voltage of the inverter circuit is 220V RMS with 50Hz. The varistor is connected in parallel to the input terminal to protect the remaining part of the circuit from the high voltage. A fuse is also connected to the phase or neutral line in against high-current faults (~3A) which may occur during the phase-neutral current cycle. In order to rectify the AC voltage, a full-wave bridge rectifier is used.

#### 3.2. DC Bus Voltage Reading Circuit

The DC bus voltage provides the current required by the motor speed and load. The average voltage is given to the motor phase windings with power switches. The voltage fluctuations must be taken into account while controlling the motor, otherwise the motor speed may oscillate. Therefore, the DC bus voltage is measured and then included in the closed loop speed control.

### 3.3. Switched Mode Power Supply (SMPS)

In general, the DC power supplies are used to obtain a tuned and regulated DC voltages. The SMPS Buck converter [25], which is designed for the drive circuit, provides DC voltage for the gate drive circuit and the linear voltage regulator.

### 3.4. Gate Driver Circuit

The microcontroller drive voltage level is not adequate to drive the power switches. Therefore, these signals must be boosted. Switches are converted to conducting state by the bootstrap topology. The signal voltage (5V) from the microcontroller is reached to the voltage level (~15V) to drive the power switches. While this method is simple and effective, there are some limitations explained in [26].

### 3.5. Power Switches for Motor Drive

While the power switches are in the conducting or cut off states, the average voltage is applied to the motor phases. When selecting the power switches (IGBTs) for application, the motor current and switch overheating must be taken into account.

### 3.6. Back EMF Circuit

It is possible to observe the back-EMF effect on the phase windings while the motor is rotating as shown in Figure 5. A modulated voltage is obtained at the motor phase terminal for a given frequency depending on the motor speed. By filtering the sum of the voltage applied to the winding using PWM and the voltage (back-EMF) caused by the rotation, the signal will form the basis for commutation.

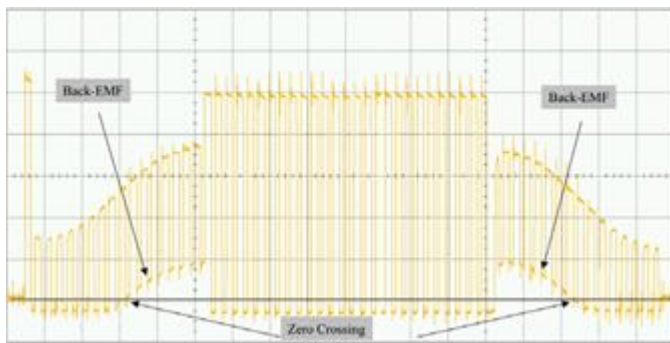
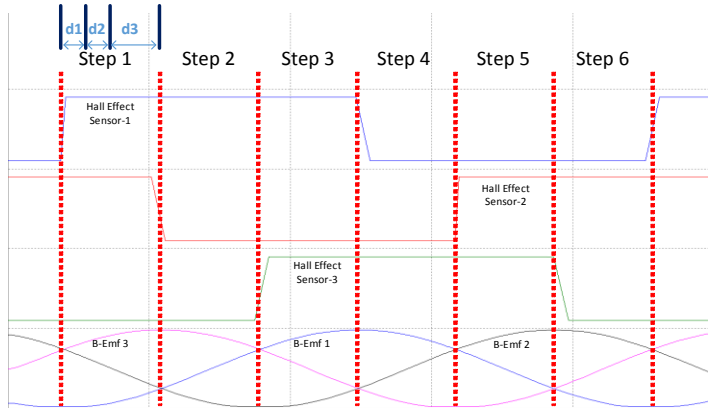


Figure 5. PMSM Motor Phase Voltage with PWM

### 3.7. Phase Shifting Circuit

The shift amount of the phase shift circuit consisting of the analog circuit elements must be adapted according to motor electrical frequency. Because as the motor speed increases, the frequencies of the measured signals will also increase. Therefore, the required amount of the shift is valid for a certain speed or speed range. When the shift rate of the motor phase voltages according to the motor speed is not properly regulated, the commutation signals will move away from the required outputs and this will have a negative effect on the inverter efficiency. This means that the currents will be applied in the wrong places relative to the back-EMF. The cut off

frequency of the low pass filter is important when filtering because, the filtered signals must give the direct commutation points.



**Figure 6.** Phase shifts between commutation intervals

d1: The phase difference between the back EMF and the reduced voltages by the three phase motor voltages

$$d1 \approx 5(R_{th2}C_4) \tag{4}$$

d2: Time delay from the low-pass filter applied to the three-phase virtual hall sensor signals obtained after the comparator circuit

$$d2 \approx 5(R_k C_k) \tag{5}$$

d3: Time delay of the phase shift circuit to adapt the commutation signal to the motor electrical frequency.

$$d3 \approx 5(R_{th2}C_d) \tag{6}$$

Cd is defined in Equation 9 by extracted Equation 7 and 8. During the calculation, collector-emitter capacitance and resistance effect of the serial connected transistor is neglected.

$$d1 + d2 + d3 \approx \frac{1}{6t_r} \tag{7}$$

$$d3 \approx \frac{1}{6t_r} - (d1 + d2) \tag{8}$$

$$C_d \approx \frac{1}{5R_{th}} \left[ \frac{1}{6t_r} - [5(R_{th2}C_4 + R_k C_k)] \right] \tag{9}$$

### 3.8. Comparator Circuit

The 3-phase waveforms obtained from the phase shifting circuits are passed through the comparator circuit. 50% duty cycle and electrical phase difference of 120° between each other occur square wave signals. These signals carry the position information of the PMSM for the 6-step speed control method with the four-switch inverter topology.

The virtual Hall Effect signal outputs resulting from the filtering and comparison processes cause missing in the ideal commutation point being synchronized with the back-EMF because of phase shifting. Therefore, there is a time difference (one commutation) between the current motor position and the virtual Hall Effect signals.



### 3.9. Microcontroller

Microcontrollers perform tasks by generation of drive signals for the PMSM in the closed-loop control process. In the proposed system, the main aim of the microcontroller is

- To create commutation points from signals from the comparison circuit
- To generate the drive signals at the switching frequency
- To perform closed loop control calculations according to DC bus voltage changes
- To calculate motor speed and speed reference
- To generate controlled PWM signals

### 4. PMSM DRIVE STAGE - EMBEDDED SOFTWARE DESIGN

The overall embedded software structure is summarized in this section. The embedded software is based on three levels: Application Layer, Motor Control Layer, Hardware Control Layer as shown in Figure 7. State diagram and the status descriptions for motor control operations are given in Figure 8 and Table 4. In this study, Atmel Atmega 328 and IAR Embedded Workbench for Atmel AVR 6.10 were used as a microcontroller and the software development environment respectively.

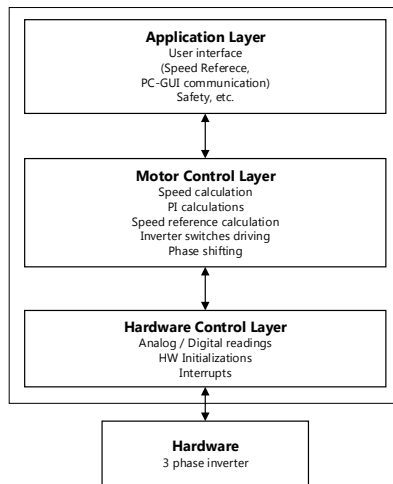


Figure 7. Embedded software structure

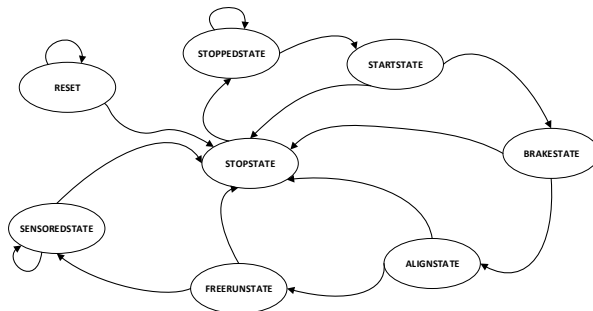


Figure 8. State diagram for motor control operations

#### 4.1. Application Layer

Motor speed reference detection and motor speed calculation, safety, position detection, commutation, control etc. are performed in Application layer. The speed reference information is constantly updated to allow the motor reaching at the required speed or stop while the motor is stationary or rotating at a certain speed. The speed reference information generated by an external circuit is isolated by the optical circuit elements on the inverter as shown in Figure 9. The hardware and the software precautions are taken to prevent malfunctions and undefined operations that may occur in the motor or inverter.

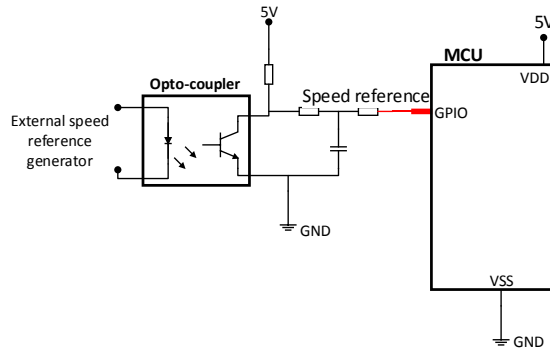


Figure 9. Speed Reference Connection

In the PMSM closed-loop control, the limit control is performed with predefined minimum and maximum values of the motor speed at certain periods. If the operating speed of the motor is too low or too high, the motor is stopped and entered the error state due to the system safety. The power consumption at the motor driving stage is measured for motor overload protection. The power limits are determined depending on the various operating motor speed ranges. During the closed-loop operation of the motor, it is checked whether the power control has been exceeded for a certain period of time according to these limits.

#### 4.2. Motor Control Layer

In motor control layer, motor speed calculations are performed in the closed loop control. Microcontroller interrupts and timers are adjusted to obtain the period during the electrical rotation of the motor.

The speed of a 3-phase motor in rpm is calculated by Equation 10. In the equation the current frequency and the number of poles are defined as  $f$  and  $p$  ( $p = 8$ ) respectively.

$$n_{rpm} = \frac{120 \times f}{p} \quad (10)$$

Speed errors are calculated from the motor speed and current reference speed using the PI controller on the microcontroller. In the closed loop operation phase, a `PI_account()` function is called up every 20ms in the main loop of the software. PI coefficients  $k_p$ ,  $k_i$  are calculated by the following equations. In these equations, the current speed reference, motor speed and speed error are expressed by  $current\_ref\_rpm$ ,  $n_{rpm}$ ,  $e(n)$  respectively.

**Table 4.** Status descriptions for motor control operations

Conditions	Motor Working Status
Speed Reference >0	STARTSTATE
If the counters' current offset value reaches the limit value	BREAKSTATE
If the time is up for bootstrap capacitor charging	ALIGNSTATE
If the counters' reaches its limit value during the aligning of the rotor	FREERUNSTATE
If the counters' reaches its limit value during the open loop	SENSOREDSTATE
Stop command is active, disabling PWM outputs	STOPPEDSTATE
System init ; Speed reference ==0; Error flag ==1	STOPSTATE

$$e(n) = current\_ref\_rpm - n_{rpm} \tag{11}$$

$$\Delta duty\_cycle(n) = \frac{k_1 \cdot e(n) - k_2 \cdot e(n-1)}{2^{PI\_GAIN}} \tag{12}$$

$$\frac{k_1 \cdot e(n) - k_2 \cdot e(n-1)}{2^{PI\_GAIN}} = k_i \cdot e(n) + k_p [e(n) - e(n-1)] \tag{13}$$

$$k_p = \left[ \frac{k_2}{2^{PI\_GAIN}} \right] \tag{14}$$

$$k_i = \left[ \frac{k_1 - k_2}{2^{PI\_GAIN}} \right] \tag{15}$$

## 5. EXPERIMENTAL RESULTS

Experimental studies for position detection and speed control of the PMSM with the four switch inverter topology were carried out. The power switching frequency is set as 7 kHz. The position detection signals were obtained from the comparator to perform a commutation similar to the Hall Effect sensor. The virtual hall effect signal outputs are composed of approximately 120° electrical phase and 50% duty cycle. The control and commutation process in the circuit were performed to generate the PWM outputs for the motor rotating at constant speed. Oscilloscope screen of three phase PMSM back-emf measurement is given in Figure 10. Reduced motor phase terminal voltages, virtual Hall Effect signal outputs for position detecting, motor phase currents and PWM signal for IGBTs are seen in Figure 11 and Figure 12

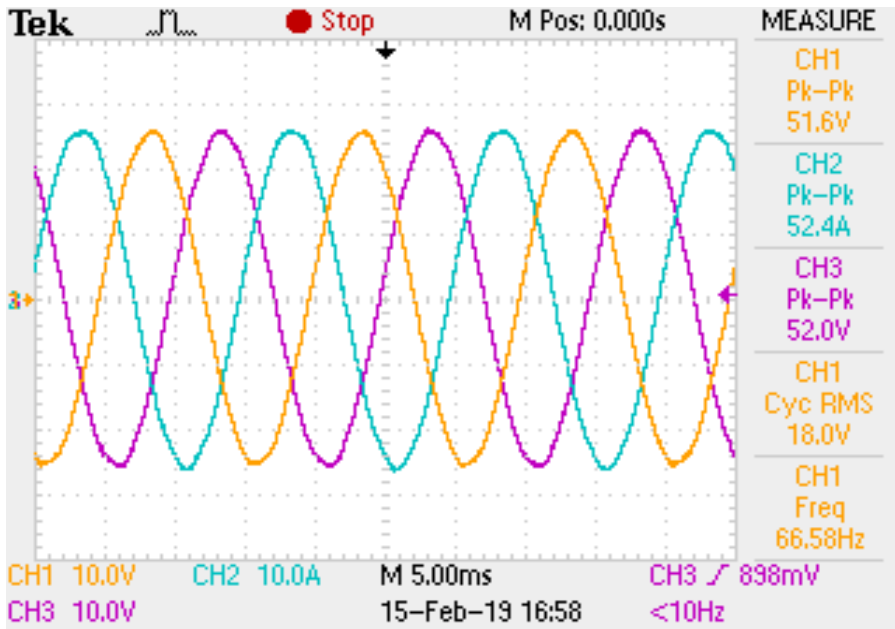


Figure 10. 3 phase PMSM back-emf measurement oscilloscope screen

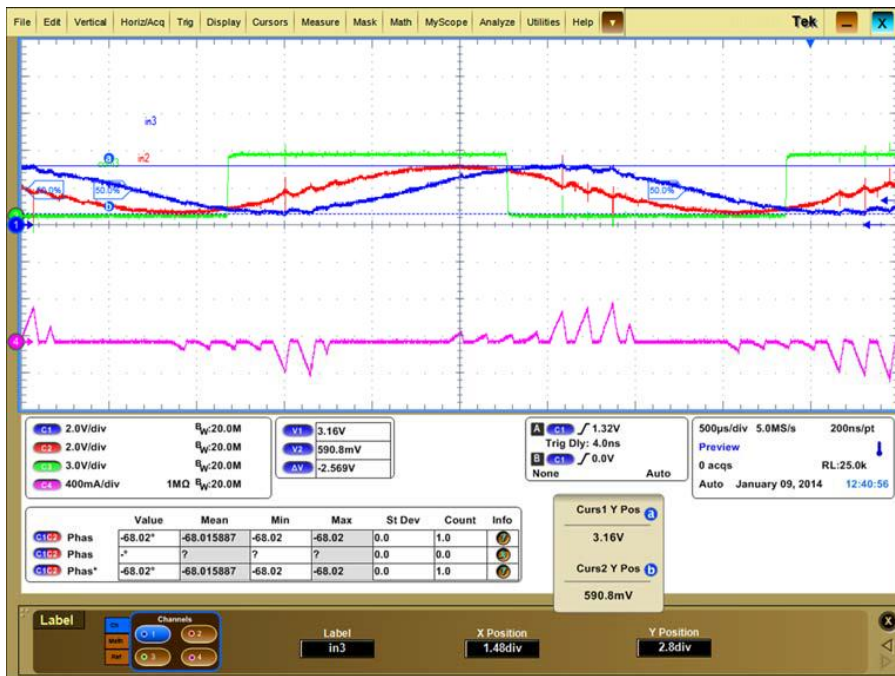


Figure 11. Reduced motor phase terminal voltages (red:IN2, blue:IN3), virtual hall effect signal outputs (green: COM3), motor phase current (pink)

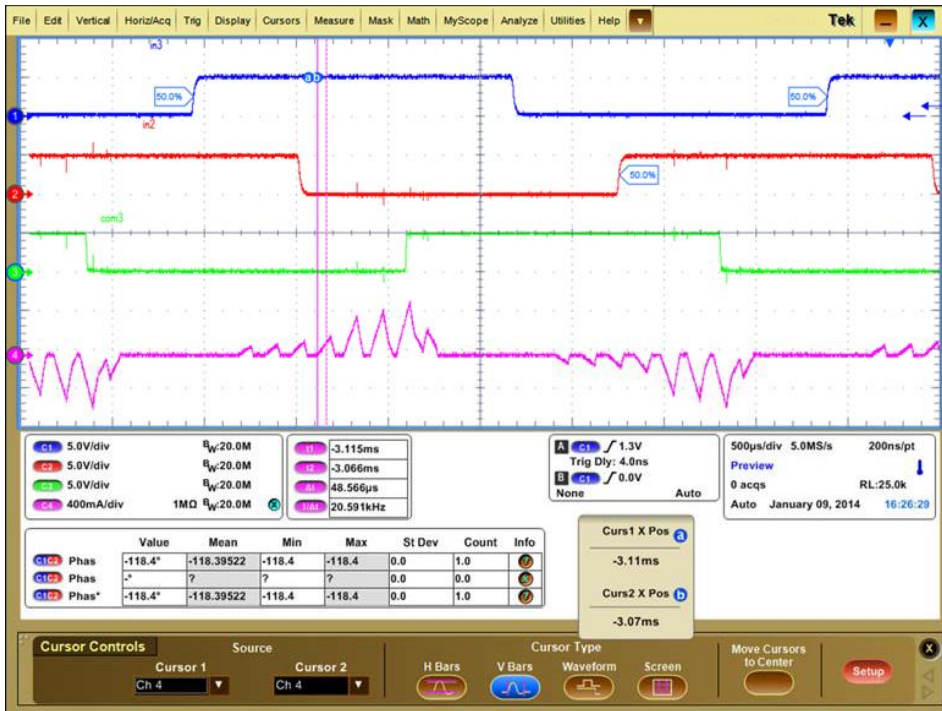


Figure 12. Virtual hall effect signal outputs (blue: COM1,red: COM2, green: COM3) ve motor phase current (pink)

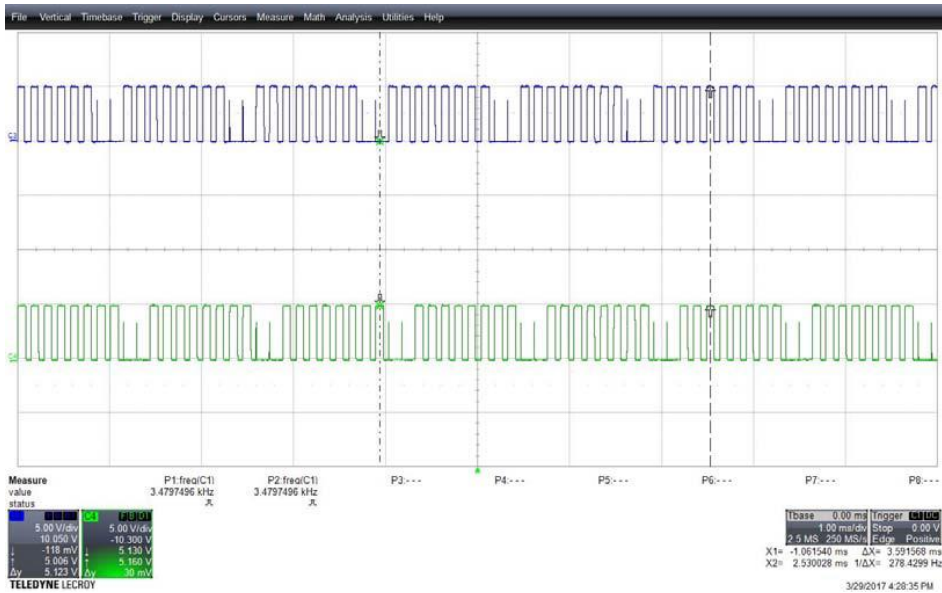


Figure 13. PWM outputs for inverter power switches

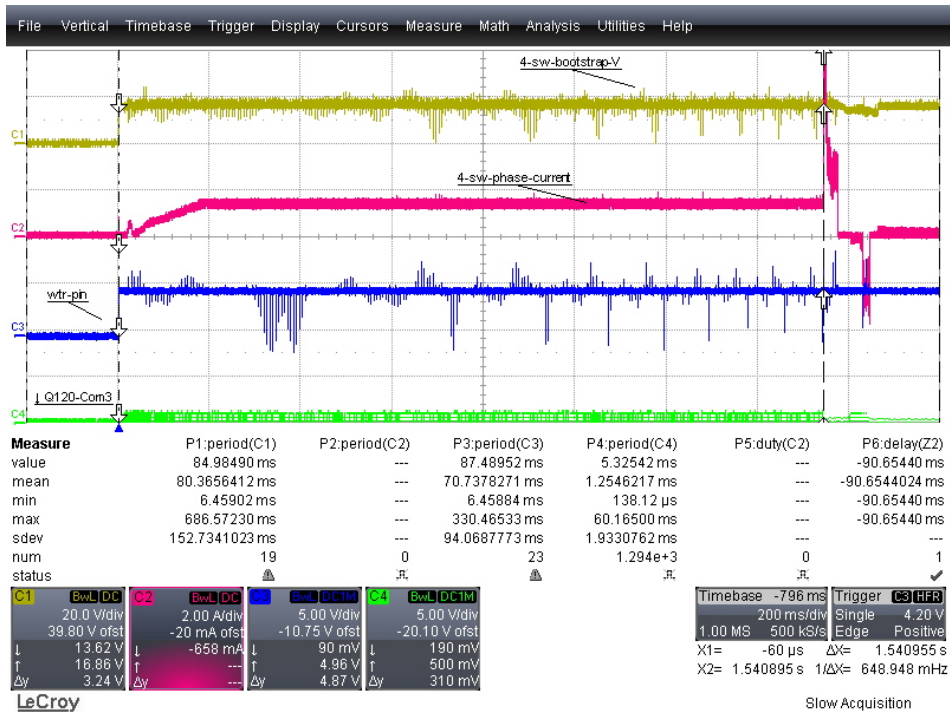


Figure 14. Bootstrap capacitor voltage (yellow), motor phase current at start-up (pink), motor start signal for system start-up check (blue), N/A(green)

## 6. CONCLUSIONS

In this work, sensorless PMSM motor position detection was achieved with six switching points for four switch inverter circuit. Since the commutation transition points follow the Virtual Hall Effect sensor signals in the method used, the 30° electrical phase shift is not required as in the methods based on the back-EMF voltage. The shifting is performed depending on the delay of the filters and motor speed. The motor terminal voltages are used directly according to the ground point of the circuit without the need for a neutral point. Thus, while a PMSM motor is driven with four switches and 6-step control method, the sensorless position detection is performed which provides position information to the closed loop speed control. Furthermore, the circuit topology with the control strategy performed in the study can be utilized in the low cost industrial applications since quantity of component for PMSM motor drive stage are reduced. According to cost analysis that is seen in the Table 5, two control method component costs are compared. Proposed method inverter layer circuit has cost effectiveness due to 4 switches vector (FOC) inverter layer circuit since its grand total price (pu) is lower.

**Table 5.** Cost comparison for 6 switches FOC vs 4 switches trapezoidal control

Components	Unit price	Q1 (pcs)	total price(pu)	Q2 (pcs)	total price(pu)
DC Bus capacitor	1,000	1	1,000	2	2,000
Gate Driver	0,670	3	2,009	2	1,339
Inverter Resistors	0,001	12	0,011	8	0,007
Inverter Diodes	0,018	6	0,106	4	0,071
Inverter power switch	0,561	6	3,368	4	2,245
Bootstrap diode	0,068	3	0,203	2	0,135
Bootstrap capacitor	0,027	3	0,080	2	0,053
Bootstrap resistor	0,001	3	0,003	2	0,002
		Grand total price (pu)	6,781	Grand total price (pu)	5,854

Q1: Quantity for 6 switch 3 phase sensorless vector (FOC) control circuit

Q2: Quantity for 4 switch 3 phase sensorless vector (FOC) control circuit

DC Bus Capacitor price (1pcs): 1pu

**REFERENCES**

[1] Joon-Hwan Lee, Sung-Chan Ahn and Dong-Seok Hyun “A BLDCM drive with trapezoidal back EMF using four-switch three phase inverter”, in Proc. IEEE Industry Applications Conference, Rome, Italy, August 2000.

[2] Changliang Xia, Zhiqiang Li and Tingna Shi “A Control Strategy for Four-Switch Three-Phase Brushless DC Motor Using Single Current Sensor”, IEEE Transactions on Industrial Electronics, Vol. 56, No.6, pp:2058 – 2066, Feb. 2009.

[3] Vanchinathan Kumarasamy and K. Vanchinathan, “Improved Performance of Four Switch Three Phase Brushless DC Motor using Speed-Current Control Algorithm”, International Journal of Computer Applications, Vol. 68, No.11, pp.1-7, April 2013.

[4] Chung-Wen Hung, Jen-Ta Su, Chih-Wen Liu, Cheng-Tsung Lin and Jhih-Han Chen “Fuzzy gain scheduling PI controller for a sensorless four switch three phase BLDC motor”, in Proc. 25 Annual IEEE Applied Power Elect. Conf. and Exposition (APEC), Palm Springs, CA, USA, March 2010.

[5] Joon-Ho Lee, Tae-Sung Kim and Dong-Seok Hyun “A study for improved of speed response characteristic in four-switch three-phase BLDC motor”, in Proc. 30th Annual Conference of IEEE Industrial Electronics Society, Busan, South Korea, Nov. 2004.

[6] A. H. Niasar, H. Moghbelli and A. Vahedi, “A low-cost sensorless control for reduced-parts, brushless DC motor drives”, in Proc. IEEE Int. Symp. on Industrial Electronics, Cambridge, UK, July. 2008.

[7] A. H. Niasar, A. Vahedi and H. Moghbelli “A Novel Position Sensorless Control of a Four-Switch, Brushless DC Motor Drive Without Phase Shifter”, IEEE Transactions on Power Electronics, Vol.23, No:6, pp.3079 – 3087, December. 2008.

[8] M. Ebadpour, M.B.B Sharifian and M.R. Feyzi, “A Simple position sensorless control strategy for four-switch three-phase brushless DC motor drives using single current sensor”, in Proc. 2nd Power Electronics, Drive Systems and Technologies Conference, 2011.

- [9] C. K. Lin, J.T. Yu and L.C. Fu, "A sensorless position control for four-switch three-phase inverter-fed interior permanent magnet synchronous motor drive systems" in Proc. 2012 IEEE/ASME International Conference on Advanced Intelligent Mechatronics (AIM), 2012.
- [10] O.C. Kivanc, S.B Ozturk, "Low-Cost Position Sensorless Speed Control of PMSM Drive Using Four-Switch Inverter". *Energies* 2019, 12, 741.
- [11] X. Liu, H. Yu, J. Yu, Y. Zhao, A Novel Speed Control Method Based on Port-Controlled Hamiltonian and Disturbance Observer for PMSM Drives, *IEEE Access*, Vol. 7, pp: 111115 - 111123, 2019.
- [12] C.T. Lin, Hung, C.-W. ve Liu, C.-W., "Position Sensorless Control for Four-Switch Three-Phase Brushless DC Motor Drives", *IEEE Tran. on Power Electronics*, Vol.23, No.1 pp. 438 – 444, 2008.
- [13] H.H. Lee, P.Q Dzung, and L.M. Phuong, "A new switching technique for Direct Torque Control of Induction Motor using Four-Switch Three-Phase Inverter with DC - link voltage imbalance", in Proc. IEEE International Conference on Industrial Technology, July 2009.
- [14] A.H. Niasar , A. Vahedi, and H. Moghbelli, "A Novel Method for Commutation Torque Ripple Reduction of Four-Switch, Three-Phase Brushless DC Motor Drive", *Iranian Journal of Electrical & Electronic Engineering*, Vol.3, No.3, pp.83-97, 2007.
- [15] G. James, K. Radhakrishnan and B. Jaya, "A Sensorless Control of Four Switch BLDC Motor Drive", *Int. Journal of Eng. Research & Tech.* Vol. 2, No. 3, pp. 1-9, March 2013.
- [16] B.K. Lee, T.H. Kim and M. Ehsani, "On the feasibility of four-switch three-phase BLDC motor drives for low cost commercial applications: topology and control", *IEEE Transactions on Power Electronics*, Vol.18, No.1, pp. 164 – 172, March 2003.
- [17] S. Ramasamy, S. Gunasekaran, S. Balasubramaniam, "A novel hybrid topology for power quality improvement using multilevel inverter for the reduction of vibration and noise in brushless DC motor for industrial applications" *Journal of Vibroengineering.*, Vol. 21 Issue 3, pp.736-759, 2019.
- [18] A.H. Niasar, A. Vahedi, and H. Moghbelli, "Design and Implementation of Sensorless Control for Four-Switch, Three-Phase Brushless DC Motor Drive Based on DSP Technology", *Iranian Journal of Electrical and Comp. Electronic Eng.*, Vol. 8, No. 1 pp.1-6, Winter-Spring 2009.
- [19] J. N. Apruzzese, E. Lupon, S. B. Monge, A. Conesa, J. Bordonau and G. G. Rojas FPGA-Based Controller for a Permanent-Magnet Synchronous Motor Drive Based on a Four-Level Active-Clamped DC-AC Converter, *Energies*, 11, 2639, pg:1-17, 2019.
- [20] J.D. Lee, B.G. Park, and T.S. Kim, "A simple fault detection of the open-switch damage in BLDC motor drive systems", in Proc. 7th Int. Conf. on Power Electronics, 2007.
- [21] J. D. Wei and B. Zhou, "Fault tolerant strategies under open phase fault for doubly salient electro-magnet motor drives", in Proc. International Conference on Electrical Machines and Systems, 2007.
- [22] X. Zhou, J. Sun, H. Li ; M. Lu ; F. Zeng ,PMSM Open-Phase Fault-Tolerant Control Strategy Based on Four-Leg Inverter, *IEEE Transactions on Power Electronics*, Vol.35, pp: 2799 - 2808, 2020.
- [23] P. Yedamale, "Brushless DC (BLDC) Motor Fundamentals", Application Note AN885, Microchip Technology Inc., 2003
- [24] Niasar, A.H., Moghbelli H. ve Vahedi, A., (2007). "A novel sensorless control method for four-switch, brushless DC motor drive without using any 30° Phase shifter", in Proc. International Conference on Electrical Machines and Systems, 2007.
- [25] Z. Sha, X. Wang, Y. Wang, H. Ma, "Optimal design of switching power supply", John Wiley&Sons, chap.3, 2015.



- [26] A. Merello, "Bootstrap Network Analysis: Focusing on the Integrated Bootstrap Functionality", Application Note AN-1123, International Rectifier.